University of Jyväskylä

Master's thesis

# QCD Bremsstrahlung at high energy


*Author:*
Tapani Stylman

*Supervisor:*
Tuomas Lappi


September 29, 2017


UNIVERSITY OF JYVÄSKYLÄ
DEPARTMENT OF PHYSICS

**Abstract**

The goal of this work is to calculate with two different methods the high energy limit of the tree-level differential cross section for a bremsstrahlung process where a quark scatters from an external Coulomb field and emits a gluon. The cross section is first calculated using "ordinary" perturbative quantum chromodynamics with the external field being that of a lepton. The matrix element for the scattering is constructed from the two related Feynman diagrams and the calculation of the cross section then proceeds straightforwardly with the methods taught in any basic particle physics course. The high energy limit is given by selecting only the terms in the matrix element that have the highest power of the center of mass momentum.

Second, the process is calculated in light cone perturbation theory. The method used in this work closely follows that of Bjorken, Kogut and Soper's QED calculation [4]. The interacting initial and final states are expanded into series of Fock states with the aid of light cone wave functions and the amplitude is calculated using "old-fashioned" Hamiltonian perturbation theory. The high energy limit is present with the choice of light-cone coordinates and in the eikonal approximation for the scattering.

**Tiivistelmä**

Tämän työn tavoitteena on laskea kahdella tavalla puutason differentiaalisen vaikutusalan korkeaenergiaraja jarrutussäteilyprosessille, jossa kvarkki siroaa ulkoisesta Coulombin kentästä ja emittoi gluonin. Ensin vaikutusala lasketaan käyttämällä "tavallista"perturbatiivista kvanttiväridynamiikkaa tapauksessa, jossa ulkoista kenttää vastaa sironta leptonista. Sirontaan liittyvä matriisielementti rakennetaan prosessiin liittyvistä kahdesta Feynmanin diagrammista, ja differentiaalisen vaikutusalan laskeminen tästä on suoraviivaista tavallisen hiukkasfysiikan alkeiskurssin tiedoilla. Korkeaenergiaraja saadaan poimimalla matriisielementistä vain voimakkaimmin massakeskipisteliikemäärästä riippuvat termit.

Toiseksi prosessi lasketaan valokartioperturbaatioteorian avulla. Tässä työssä käytetty menetelmä noudattelee pitkälti Bjorkenin, Kogutin ja Soperin vastaavaa QED-laskua [4]. Prosessin vuorovaikuttavat alku- ja lopputilat kehitetään valokartioaaltofunktioden avulla sarjoiksi Fockin avaruuden tiloja ja amplitudi lasketaan "vanhanaikaisilla"hamiltonilaisen perturbaatioteorian keinoilla. Korkeaenergiaraja on luontevasti näkyvissä valokartiokoordinaatiston valinnassa ja sironnan eikonaaliapproksimaatiossa.

# Contents

# 1 Introduction

Because of the curious behaviour of the strong coupling, perturbative quantum chromodynamics only gives meaningful results at very high energies. Therefore various ultrarelativistic approximations are part and parcel of most perturbative QCD calculations. Quantizing the field theory on the light-cone rather than at equal time leads to a natural high momentum limit for the theory and exhibits many useful traits that simplify some calculations significantly.

In practice this means selecting a particular system of coordinates and applying the methods of Hamiltonian perturbation theory. This framework, originally coined by Dirac as the front form of Hamiltonian dynamics [1], has since been reintroduced under many different names such as light-cone quantization, light-front quantization, null-plane quantization [2] or light-cone perturbation theory, all effectively reiterating the same ideas. This thesis shall refer to it as light-cone perturbation theory, or LCPT for short.

A very useful feature of LCPT is that the ground state of the free theory is also the ground state in the interacting theory. LCPT, being 'old-fashioned' or Hamiltonian in nature, is particularly useful for the analysis of (hadronic) bound states, whereas the now ubiquitous action based method excels in the calculation of cross sections [2].

The objective of this thesis is to go through the calculation of a tree-level high energy bremsstrahlung scattering cross section for a process that involves a high energy quark scattering off an electromagnetic Coulomb potential and emitting a gluon (see figure 1). The final state quark and gluon, while taken to be on mass shell as external particles, would of course quickly undergo

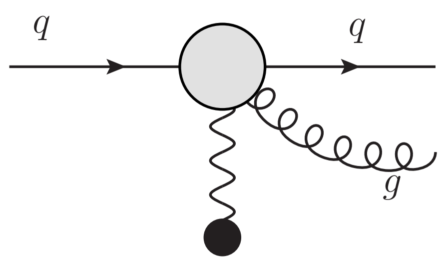


Figure 1: A diagrammatic representation of the scattering process.

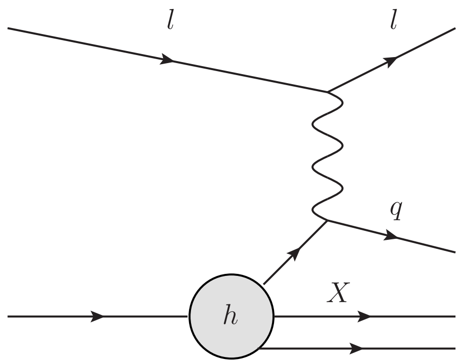


Figure 2: Parton model deep inelastic scattering at leading order.

hadronization due to color confinement, whereas the incoming quark should be thought of as a parton within an existing hadron.

The process has an obvious connection to the experimentally significant process of Deep Inelastic Scattering (DIS), where a high energy lepton probes a hadron with a virtual photon (see figure 2). The bremsstrahlung process is one of the so-called real emission corrections that need to be considered alongside with the loop diagrams when calculating the next-to-leading-order amplitudes for DIS.

The DIS experiments were performed in the 1960s and 70s at the Stanford Linear Accelerator Center (SLAC). The electrons, when fired at hydrogen targets, exhibited primarily hard scatterings from the protons and in most cases shattered the target producing a shower of outgoing hadrons. This led James Bjorken and Richard Feynman to the discovery of the parton model: the proton should be considered a loosely bound collection of constituent fermions that carry electric charge and other electrically neutral particles that hold the proton together.

It was also discovered that the structure of the proton looked almost completely independent of the energy it was probed at, i.e. that the partons would essentially not be able to interact with each other during the short time scales of the deep inelastic regime. This property came to be known as Bjorken scaling. While this behaviour is simple and elegant, it proved difficult to reconcile with established quantum field theory in the 70s. The partons would have to exhibit asymptotic freedom, while there was no way for any known type of theory to have such a property. The answer was given by ’t Hooft, Politzer, Gross and Wilczek with their discovery of non-Abelian gauge theory. Generalizing the concept of local gauge invariance beyond that of the simple local phase rotation symmetry of QED to permit any kind of continuous symmetry gave rise to Yang-Mills theory and modern quantum chromodynamics.

Perurbative QCD deals with free quark and gluons, and their scatterings are usually readily modelled with the tools of regular perturbation theory. In the context of DIS, however, the quarks are *not* free, but part of a bound state, the proton. Accurately modelling DIS thus requires a different approach and a different physical picture of the process. There are many possible solutions to the problem, and one of them is given by LCPT.

The motivation behind this thesis is trying to understand the connection between two fundamentally different descriptions of the same process: regular pQCD and LCPT. To that end, instead of analysing the complete DIS cross section, we focus on just the bremsstrahlung process. The cross section is first calculated using the more familiar action-derived, or Lagrangian, Feynman diagram method, and then again using the tools of LCPT.

The process involves a quark scattering in an external electromagnetic Coulomb field. When calculating the cross section with the Feynman diagram method the external field is replaced by a lepton. In the high energy limit the lepton ends up looking just like a source for the external Coulomb field. The LCPT method, on the other hand, deals with the external field by explicitly adding it in the equation of motion for the quark [4].

A very novel feature in the LCPT calculation is the use of so-called light-cone wave functions when describing the interacting states. The initial (quark) and final (quark-gluon) states are decomposed into a series of Fock states, i.e. states with fixed numbers of particles, the weight of each term being given by a corresponding wave function describing the amplitude for the interacting hadron state to fluctuate into that particular combination of particles [5]. For the leading order result only two terms in these series need to be considered and the wave functions themselves are only evaluated to leading order.

The structure of the thesis is as follows. In section 2 the cross section is calculated in the more familiar method, constructing the matrix element from the Feynman diagrams and performing the high energy approximations. Section 3 covers the corresponding LCPT calculation starting from a brief introduction to the basic conventions and ideas. Section 4 outlines the application

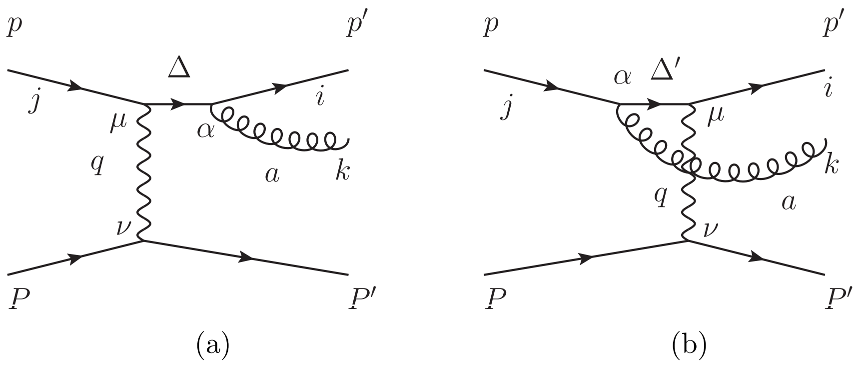


Figure 3: The two leading order Feynman diagrams. The symbols $p$, $p'$, $k$, $\Delta$, $\Delta'$, $P$ and $P'$ label the momenta, $i$, $j$ and $k$ are quark color indices, $a$ is the gluon color index and $\alpha$, $\mu$ and $\nu$ are the Lorentz indices related to the vertices.

of these ideas and methods to scatterings with color charged targets and the additional complications involved. In section 5 the results are discussed and a few thoughts are given to the application of these ideas and techniques in current research.

# 2 Calculation using normal Feynman rules

## 2.1 The matrix element

The process can be thought of as the large momentum 2 to 3 scattering of a quark off a lepton while emitting a gluon. Since the lepton does not couple with gluons, at tree-level there are only two contributing Feynman diagrams, represented by figures 3a and 3b. The matrix element corresponding to the first figure is

$$\begin{aligned} i\mathcal{M}_I &= \bar{u}(p')(ig\gamma^\alpha(T^a_{ij}))\epsilon^*{}_\alpha(k)\frac{i\not{\Delta}}{\Delta^2 + i\epsilon}(ieQ\gamma^\mu)u(p)\frac{-ig_{\mu\nu}}{q^2}\bar{u}(P')(-ie\gamma^\nu)u(P) \\ &= i\frac{gQe^2T^a_{ij}}{q^2(\Delta^2 + i\epsilon)}\epsilon^*{}_\alpha(k)\bar{u}(p')\gamma^\alpha\not{\Delta}\gamma^\mu u(p)\bar{u}(P')\gamma_\mu u(P), \end{aligned} \quad (1)$$

where the quark is taken to be massless, $m$ is the mass of the lepton and $Q$ is the electric charge of the quark. The second diagram gives similarly

$$i\mathcal{M}_{II} = i\frac{gQe^2T^a_{ij}}{q^2(\Delta'^2 + i\epsilon)}\epsilon^*{}_\alpha(k)\bar{u}(p')\gamma^\mu \not{\Delta}'\gamma^\alpha u(p)\bar{u}(P')\gamma_\mu u(P). \quad (2)$$

From four-momentum conservation it follows that $\Delta = p' + k$, $\Delta' = p - k$ and $P' = p + P - p' - k$.

The squared and spin sum-averaged matrix element is thus

$$\overline{|\mathcal{M}|}^2 = \frac{1}{2}\frac{1}{2}\frac{1}{3}\frac{g^2Q^2e^4}{q^4}C\left[\frac{1}{(\Delta^2)^2}Q_1^{\mu\nu} + \frac{1}{\Delta^2\Delta'^2}Q_2^{\mu\nu} + \frac{1}{\Delta^2\Delta'^2}Q_3^{\mu\nu} + \frac{1}{(\Delta'^2)^2}Q_4^{\mu\nu}\right]L_{\mu\nu}, \quad (3)$$

where $C$ is the color factor

$$C = T^a_{ij}(T^a_{ij})^* = T^a_{ij}T^a_{ji} = \mathrm{Tr}[T^aT^a] = \frac{1}{2}\delta^{aa} = 4, \quad (4)$$

$L_{\mu\nu}$ is the lepton trace

$$L_{\mu\nu} = \mathrm{Tr}\big[(\not{P} + m)\gamma_\mu(\not{P}' + m)\gamma_\nu\big] = 4\left[P_\mu P'_\nu + P_\nu P'_\mu + (4m^2 - (P\cdot P'))g_{\mu\nu}\right] \quad (5)$$

and the $Q_i^{\mu\nu}$'s are the four quark traces

$$\begin{aligned} Q_1^{\mu\nu} &= -\,\mathrm{Tr}\big[\not{p}\gamma^\mu\not{\Delta}\gamma^\alpha\not{p}'\gamma_\alpha\not{\Delta}\gamma^\nu\big] \\ Q_2^{\mu\nu} &= -\,\mathrm{Tr}\big[\not{p}\gamma^\alpha\not{\Delta}'\gamma^\mu\not{p}'\gamma^\nu\not{\Delta}'\gamma_\alpha\big] \\ Q_3^{\mu\nu} &= -\,\mathrm{Tr}\big[\not{p}\gamma^\mu\not{\Delta}\gamma^\alpha\not{p}'\gamma^\nu\not{\Delta}'\gamma_\alpha\big] \\ Q_4^{\mu\nu} &= -\,\mathrm{Tr}\big[\not{p}\gamma^\alpha\not{\Delta}'\gamma^\mu\not{p}'\gamma_\alpha\not{\Delta}\gamma^\nu\big]. \end{aligned} \quad (6)$$

Note that the $i\epsilon$'s in the denominators have been suppressed in equation (3) for clarity of notation. They will not be needed anyway.

The quark traces are traces of eight gamma matrices. Using the well known properties

$$\gamma_\alpha\gamma^\mu\gamma^\alpha = -2\gamma^\mu \quad (7)$$

and

$$\gamma_\alpha\gamma^\mu\gamma^\nu\gamma^\rho\gamma^\alpha = -2\gamma^\rho\gamma^\nu\gamma^\mu \quad (8)$$

the number of gamma matrices reduces to six in each trace:

$$
\begin{aligned}
Q_1^{\mu\nu} &= 2\,\mathrm{Tr}\big[\not{p}\gamma^\mu \not{\Delta}\not{p}'\not{\Delta}\gamma^\nu\big] \\
Q_2^{\mu\nu} &= 2\,\mathrm{Tr}\big[\not{p}\not{\Delta}'\gamma^\mu \not{p}'\gamma^\nu\not{\Delta}'\big] \\
Q_3^{\mu\nu} &= 2\,\mathrm{Tr}\big[\not{\Delta}\gamma^\mu \not{p}\not{p}'\gamma^\nu\not{\Delta}'\big] \\
Q_4^{\mu\nu} &= 2\,\mathrm{Tr}\big[\not{p}\not{p}'\gamma^\mu \not{\Delta}'\not{\Delta}\gamma^\nu\big].
\end{aligned} \tag{9}
$$

The generic six-gamma trace can be straightforwardly, if tediously, evaluated using the Clifford algebra,

$$
\left\{\gamma^\alpha, \gamma^\beta\right\} = \gamma^\alpha\gamma^\beta + \gamma^\beta\gamma^\alpha = 2g^{\alpha\beta}, \tag{10}
$$

and the usual properties of traces, yielding

$$
\begin{aligned}
\mathrm{Tr}\big[\gamma^\alpha\gamma^\beta\gamma^\gamma\gamma^\delta\gamma^\epsilon\gamma^\zeta\big] = 4\,&\big[g^{\alpha\beta}\left(g^{\gamma\delta}g^{\epsilon\zeta} - g^{\gamma\epsilon}g^{\delta\zeta} + g^{\gamma\zeta}g^{\delta\epsilon}\right) - g^{\alpha\gamma}\left(g^{\beta\delta}g^{\epsilon\zeta}\right. \\
&\left.-g^{\beta\epsilon}g^{\delta\zeta} + g^{\beta\zeta}g^{\delta\epsilon}\right) + g^{\alpha\delta}\left(g^{\beta\zeta}g^{\gamma\epsilon} - g^{\beta\epsilon}g^{\gamma\zeta} + g^{\beta\gamma}g^{\epsilon\zeta}\right) - g^{\alpha\epsilon}\left(g^{\beta\zeta}g^{\gamma\delta}\right. \\
&\left.-g^{\beta\delta}g^{\gamma\zeta} + g^{\beta\gamma}g^{\delta\zeta}\right) + g^{\alpha\zeta}\left(g^{\beta\epsilon}g^{\gamma\delta} - g^{\beta\delta}g^{\gamma\epsilon} + g^{\beta\gamma}g^{\delta\epsilon}\right)\big]\,.
\end{aligned} \tag{11}
$$

Applying this to our traces we get

$$
\begin{aligned}
Q_1^{\mu\nu} =& 16(k\cdot p')\,[p^\mu k^\nu + p^\nu k^\mu - (k\cdot p)g^{\mu\nu}] \\
Q_2^{\mu\nu} =& 16(k\cdot p)\,[p'^\mu k^\nu + p'^\nu k^\mu - (k\cdot p')g^{\mu\nu}] \\
Q_3^{\mu\nu} =& 16[(p\cdot p')(g^{\mu\nu}[(k\cdot p) - (k\cdot p') + (p\cdot p')] + k^\mu p'^\nu) + p^\mu[p^\nu(k\cdot p') \\
&- (k^\nu + p'^\nu)(p\cdot p')] - p'^\mu[p'^\nu(k\cdot p) + p^\nu[(k\cdot p) - (k\cdot p') + (p\cdot p')]]] \\
Q_4^{\mu\nu} =& 16[(p\cdot p')(g^{\mu\nu}[(k\cdot p) - (k\cdot p') + (p\cdot p')] - k^\mu p^\nu) + p'^\mu[p'^\nu(k\cdot p). \\
&+ (p^\nu - k^\nu)(p\cdot p')] + p^\mu[p^\nu(k\cdot p') - p'^\nu[(k\cdot p) - (k\cdot p') + (p\cdot p')]]].
\end{aligned} \tag{12}
$$

After contracting the traces and performing some simplifying algebra, one gets the still somewhat daunting result

$$
\overline{|\mathcal{M}|}^2 = -\frac{1}{2}\frac{1}{2}\frac{1}{3}g^2Q^2e^4C\frac{1}{(k\cdot p)(k\cdot p')((k\cdot p) - (k\cdot p') + (p\cdot p'))^2}8\Big[(k\cdot p)^2
\Big[(k\cdot p) + m^2 - (p\cdot P) + (P\cdot p')\Big] - 2(k\cdot p)\Big[(k\cdot P)\Big((p\cdot P) - (p\cdot p')\Big) -
(p\cdot p')\Big(m^2 - (p\cdot P) + (P\cdot p')\Big) + (P\cdot p')\Big((p\cdot P) + (P\cdot p')\Big)\Big] + (k\cdot p')^2
\Big[(k\cdot P) + m^2 - (p\cdot P) + (P\cdot p')\Big] + 2(k\cdot p')\Big[-(p\cdot p')\Big((k\cdot P) + m^2
$$

$$
+ (P\cdot p')\Big) - (k\cdot P)(P\cdot p') + (p\cdot P)\Big((p\cdot p') + (P\cdot p')\Big) + (p\cdot P)^2\Big]
+ 2(p\cdot p')\Big[(k\cdot P)\Big( - (p\cdot P) + (p\cdot p') + (P\cdot p')\Big) + (p\cdot p')\Big(m^2 - (p\cdot P)
+ (P\cdot p')\Big) - 2(p\cdot P)(P\cdot p')\Big]\Big]. \tag{13}
$$

## 2.2 The high-energy limit

Next we are tasked with examining the high energy behaviour of this expression. We are interested specifically in the scattering where the analogue to the Mandelstam $s$ of 2 to 2 scattering, the invariant $S = (p + P)^2$, is large and the product $p \cdot P$ in particular is very large. In this limit $S \approx 2p \cdot P$.

We know that $P - P' = p' + k - p$. Taking the dot product with $P$ on both sides gives $P^2 - P' \cdot P = p' \cdot P + k \cdot P - p \cdot P$. Because we are interested specifically in the limit where $p \cdot P$ is very large, this leads to

$$
p\cdot P \approx p'\cdot P + k\cdot P. \tag{14}
$$

We can then write $2p \cdot P = S$, $2P \cdot p' = (1 - z)S$ and $2P \cdot k = zS$. Using these the high energy matrix element simplifies to

$$
\begin{aligned}
\overline{|\mathcal{M}|}^2 \approx& -\frac{1}{3}g^2Q^2e^4\frac{8}{(k\cdot p)(k\cdot p')((k\cdot p) - (k\cdot p') + (p\cdot p'))^2}\Big[ - 2(k\cdot p)\\
&\times \Big[(k\cdot P)(p\cdot P) + (P\cdot p')\Big((p\cdot P) + (P\cdot p')\Big)\Big] + 2(k\cdot p')\Big[ - (k\cdot P)\\
&\times (P\cdot p') + (p\cdot P)\Big((P\cdot p')\Big) + (p\cdot P)^2\Big] + 2(p\cdot p')\Big[(k\cdot P)\Big( - (p\cdot P)\\
&+ (P\cdot p')\Big) - 2(p\cdot P)(P\cdot p')\Big]\Big]\\
=& \frac{4}{3}g^2Q^2e^4\frac{S^2(z^2 - 2z + 2)}{(k\cdot p)(k\cdot p')((k\cdot p) - (k\cdot p') + (p\cdot p'))}.
\end{aligned} \tag{15}
$$

Note that all dependence on the lepton mass $m$ has disappeared at this limit.

In the following we will be using the so-called light-cone variables: for any four-vector $\bar{v} = (v^0, v^1, v^2, v^3)$ we can define the vector in light-cone coordinates as $\bar{v} = (v^+, v^-, v^1, v^2)$ with $v^+ = 2^{-\frac{1}{2}}(v^0 + v^3)$ and $v^- = 2^{-\frac{1}{2}}(v^0 - v^3)$. The transverse components $v^1$ and $v^2$ are usually collectively referred to as

$\bar{v}_\perp$. The dot product is given by the metric

$$g_{\mu\nu} = C^\alpha{}_\mu \hat{g}_{\alpha\beta} (C^{-1})^\beta{}_\nu = \begin{pmatrix} 0 & 1 & 0 & 0 \\ 1 & 0 & 0 & 0 \\ 0 & 0 & -1 & 0 \\ 0 & 0 & 0 & -1 \end{pmatrix}. \tag{16}$$

The expression in (15) is still independent of frame. Fixing the frame such that the incoming quark has a large momentum in the positive $z$ direction and the lepton has large momentum in the negative $z$-direction is equivalent to the quark having large $p^+$ and small $p^-$, and the lepton in turn having large $P^-$ and small $P^+$. In such a frame equation (14) leads to $p^+ = k^+ + p'^+$ and allows us to also write $k^+ = zp^+$ and $p'^+ = (1-z)p^+$. In this frame the expression for the squared matrix element of equation (15) simplifies to

$$\overline{|\mathcal{M}|}^2 \approx \frac{32}{3} g^2 Q^2 e^4 \frac{S^2(z^2 - 2z + 2)(1-z)z^2}{k_\perp^2 q_\perp^2 (k_\perp - z q_\perp)^2}. \tag{17}$$

## 2.3 The differential cross-section

The differential cross-section for a process with two particles in the initial state and three in the final state is well known:

$$\begin{aligned}
\mathrm{d}\sigma &= \frac{|\mathcal{M}|^2}{2\sqrt{\lambda(S,0,m^2)}} (2\pi)^4 \delta^{(4)}(p + P - p' - k - P') \delta(p'^2)\delta(k^2)\delta(P'^2 - m^2) \\
&\quad \times \frac{\mathrm{d}^4 p'}{(2\pi)^3} \frac{\mathrm{d}^4 k}{(2\pi)^3} \frac{\mathrm{d}^4 P'}{(2\pi)^3} \\
&\approx \frac{|\mathcal{M}|^2}{2S} (2\pi)^4 \delta^{(4)}(p + P - p' - k - P') \frac{\mathrm{d}p'^+ \mathrm{d}^2 p'_\perp}{2p'^+(2\pi)^3} \frac{\mathrm{d}k^+ \mathrm{d}^2 k_\perp}{2k^+(2\pi)^3} \frac{\mathrm{d}P'^- \mathrm{d}^2 P'_\perp}{2P'^-(2\pi)^3} \\
&= \frac{|\mathcal{M}|^2}{2S} (2\pi) \delta(p^+ + P^+ - p'^+ - k^+ - P'^+) \frac{\mathrm{d}p'^+ \mathrm{d}^2 p'_\perp}{2p'^+(2\pi)^3} \frac{\mathrm{d}k^+ \mathrm{d}^2 k_\perp}{2k^+(2\pi)^3} \\
&\quad \times \frac{1}{2(p^- + P^- - p'^- - k^-)} \\
&\approx \frac{|\mathcal{M}|^2}{2S} (2\pi) \delta(p^+ - p'^+ - k^+) \frac{\mathrm{d}p'^+ \mathrm{d}^2 p'_\perp}{2p'^+(2\pi)^3} \frac{\mathrm{d}k^+ \mathrm{d}^2 k_\perp}{2k^+(2\pi)^3} \frac{1}{2P^-} \\
&\approx \frac{|\mathcal{M}|^2}{2S^2} (2\pi) \delta(p^+ - p'^+ - k^+) p^+ \frac{\mathrm{d}p'^+ \mathrm{d}^2 p'_\perp}{2p'^+(2\pi)^3} \frac{\mathrm{d}k^+ \mathrm{d}^2 k_\perp}{2k^+(2\pi)^3}
\end{aligned} \tag{18}$$

where $\lambda(x,y,z) \equiv x^2+y^2+z^2-2xy-2xz-2yz$ and $P^- \approx \frac{S}{2p^+}$.

Inserting the squared matrix element from (17) we get the final result for the differential cross-section:

$$\begin{aligned} d\sigma = &\frac{16}{3} g^2 Q^2 e^4 \frac{z^2(1-z)(z^2-2z+2)}{k_\perp^2 q_\perp^2 (k_\perp - zq_\perp)^2} p^+(2\pi) \\ &\times \delta(p^+ - p'^+ - k^+) \frac{dp'^+ d^2 p'_\perp}{2p'^+(2\pi)^3} \frac{dk^+ d^2 k_\perp}{2k^+(2\pi)^3}. \end{aligned} \tag{19}$$

# 3 Light-cone perturbation theory calculation

## 3.1 Basic concepts and notation

We mostly follow the conventions of Kogut and Soper [3, 4]. We will be working with the light-cone variables defined in section 2.2, i.e. the coordinates related to the standard frame by

$$x^\mu = C^\mu{}_\nu \hat{x}^\nu, \tag{20}$$

where $\hat{x}^\nu$ are the coordinates in the old frame and

$$C^\mu{}_\nu = \begin{pmatrix} \frac{1}{\sqrt{2}} & 0 & 0 & \frac{1}{\sqrt{2}} \\ \frac{1}{\sqrt{2}} & 0 & 0 & -\frac{1}{\sqrt{2}} \\ 0 & 1 & 0 & 0 \\ 0 & 0 & 1 & 0 \end{pmatrix}. \tag{21}$$

Momenta in LCPT are always on-shell [5], i.e. $k^2 = 2k^+k^- - k_\perp^2 = m^2$ for any particle with momentum $k$ and mass $m$, and thus only three components of the four-vector are independent:

$$k^\mu = \left(k^+, k^-, \bar{k}_\perp\right) = \left(k^+, \frac{\bar{k}_\perp^2 + m^2}{2k^+}, \bar{k}_\perp\right). \tag{22}$$

For the gluon polarization vectors we adopt the Bjorken–Drell convention and work in the light-cone gauge $A^+ = 0$. With the requirement of transversality [6], $k_\mu \epsilon^\mu(k,\lambda) = 0$, the polarization vectors are

$$\epsilon^\mu(k,\lambda) = \left(0, \frac{\bar{\epsilon}_\perp(\lambda)\cdot \bar{k}_\perp}{k^+}, \bar{\epsilon}_\perp(\lambda)\right) \tag{23}$$

with the transverse polarization vectors

$$\bar{\epsilon}_\perp(\lambda) = \bar{\epsilon}_\perp(\pm 1) = \frac{-1}{\sqrt{2}}\,(\pm 1, i)\,. \tag{24}$$

The transverse vectors satisfy

$$\sum_\lambda \epsilon^*_{\perp i}(\lambda)\epsilon_{\perp j}(\lambda) = \delta_{ij}. \tag{25}$$

To quantize the theory on the light-cone we postulate the (anti-)commutation relations

$$\big\{a(p,s,f), a^\dagger(p',s',f')\big\} = 2p^+(2\pi)^3\delta(p^+ - p'^+)\delta^{(2)}(\bar{p}_\perp - \bar{p}'_\perp)\delta^{ss'}\delta^{ff'} \tag{26}$$

$$\big[b(k,\lambda,c), b^\dagger(k',\lambda',c')\big] = 2k^+(2\pi)^3\delta(k^+ - k'^+)\delta^{(2)}(\bar{k}_\perp - \bar{k}'_\perp)\delta^{\lambda\lambda'}\delta^{cc'} \tag{27}$$

for fermionic and bosonic operators $a$ and $b$, and define general multi-particle Fock states with $n_q$ quarks and $n_g$ gluons as

$$|n_q, p_i, s_i; n_g, k_j, \lambda_j\rangle = \prod_{i=0}^{n_q} a^\dagger(p_i, s_i) \prod_{j=0}^{n_g} b^\dagger(k_j, \lambda_j)\,|0\rangle\,, \tag{28}$$

where $|0\rangle$ is the vacuum. Thus the Fock states are normalized as

$$\langle q(p',s')|q(p,s)\rangle = 2p^+(2\pi)^3\delta(p^+ - p'^+)\delta^{(2)}(\bar{p}_\perp - \bar{p}'_\perp)\delta^{ss'}. \tag{29}$$

We should also define the field operator $\psi$ in the Fourier basis:

$$\psi(x) = \int \frac{\mathrm{d}p^+\mathrm{d}^2p_\perp}{(2\pi)^3 2p^+}\sum_s \left(e^{-ip\cdot x}a^s_p u^s(p) + e^{ip\cdot x}b^{s\dagger}_p v^s(p)\right). \tag{30}$$

The equal-$x^+$ anticommutation relations satisfied by the field operator components are

$$\{\psi_a(x), \psi^\dagger_b(y)\} = \delta_{ab}\delta(x^- - y^-)\delta^{(2)}(x_\perp - y_\perp). \tag{31}$$

Note that we are postulating the anticommutation relations at equal *light-cone* time. This is fundamentally different from the usual equal time (anti)commutation relations.

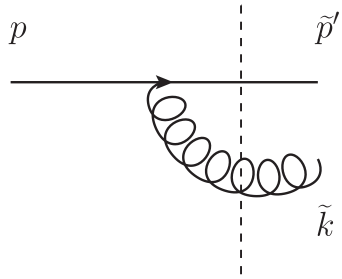


Figure 4: A diagrammatic representation of the light-cone wave function for a quark splitting into a quark-gluon pair. The dashed line indicates an intermediate state that is implied to undergo further interactions.

## 3.2 Light-cone wave functions and the Fock state expansions of interacting states

Following the conventions of [5] the light-cone wave function for a quark splitting into a quark-gluon-pair is

$$\Psi_{q\to qg}(p\to\widetilde{p}',\widetilde{k}) = g\bar{u}(\widetilde{p}')\not{\epsilon}^*(\widetilde{k})(t^a_{ij})u(p)\frac{1}{2p^+}\frac{1}{p^- - \widetilde{p}'^- - \widetilde{k}^-}. \tag{32}$$

The light-cone Fock state expansion for the interacting quark state to first order is

$$|q(p)\rangle = |q(p)\rangle_0 + \int \mathrm{d}\Omega_1 \Psi_{q\to qg}(p\to\widetilde{p}',\widetilde{k}) \left|q(\widetilde{p}')g(\widetilde{k})\right\rangle_0, \tag{33}$$

where the phase-space integral is

$$\int \mathrm{d}\Omega_1 = 2p^+(2\pi)^3 \int \sum_{\lambda,a} \frac{\mathrm{d}\widetilde{k}^+\mathrm{d}^2\widetilde{k}_\perp}{2\widetilde{k}^+(2\pi)^3} \sum_{\sigma,\alpha,f} \frac{\mathrm{d}\widetilde{p}'^+\mathrm{d}^2\widetilde{p}'_\perp}{2\widetilde{p}'^+(2\pi)^3}\delta(p^+ - \widetilde{k}^+ - \widetilde{p}'^+) \times \delta^2(p_\perp - \widetilde{k}_\perp - \widetilde{p}'_\perp). \tag{34}$$

Also required is the expansion of the interacting quark-gluon state $|q(p')q(k)\rangle$:

$$|q(p')g(k)\rangle = |q(p')g(k)\rangle_0 + \int \mathrm{d}\Omega_2 \Psi_{qg\to q}(p',k\to\widetilde{p})\,|q(\widetilde{p})\rangle_0\,, \tag{35}$$

Table 1: Matrix elements borrowed from Lepage and Brodsky[7], modified for our Kogut-Soper conventions and massless quarks. Here $\epsilon^{12} = -\epsilon^{21} = 1$ and $\epsilon^{11} = \epsilon^{22} = 0$, and $p_\perp \times p'_\perp = p^i_\perp \epsilon^{ij} {p'_\perp}^j = p^1_\perp {p'_\perp}^2 - p^2_\perp {p'_\perp}^1$.

| Matrix element | Value |
|---|---|
| $\frac{\bar{u}_{\sigma'}(p')}{\sqrt{p'^+}}\gamma^+ \frac{u_\sigma(p)}{\sqrt{p^+}}$ | $2\delta_{\sigma\sigma'}$ |
| $\frac{\bar{u}_{\sigma'}(p')}{\sqrt{p'^+}}\gamma^- \frac{u_\sigma(p)}{\sqrt{p^+}}$ | $\delta_{\sigma\sigma'}\frac{1}{p^+p'^+}(p_\perp \cdot p'_\perp - i\sigma p_\perp \times p'_\perp)$ |
| $\frac{\bar{u}_{\sigma'}(p')}{\sqrt{p'^+}}\gamma^i_\perp \frac{u_\sigma(p)}{\sqrt{p^+}}$ | $\delta_{\sigma\sigma'}\left(\frac{p'^i_\perp - i\sigma\epsilon^{ij}p'^j_\perp}{p'^+} + \frac{p^i_\perp + i\sigma\epsilon^{ij}p^j_\perp}{p^+}\right)$ |

where the phase-space integral is now

$$\int \mathrm{d}\Omega_2 = 2(p'^+ + k^+)(2\pi)^3 \int \sum_{\sigma,\alpha,f} \frac{\mathrm{d}\widetilde{p}^+ \mathrm{d}^2\widetilde{p}_\perp}{2\widetilde{p}^+(2\pi)^3}\delta(k^+ + p'^+ - \widetilde{p}^+)\delta^{(2)}(k_\perp + p'_\perp - \widetilde{p}_\perp). \tag{36}$$

Obviously the integral over the phase-space of a single particle yields little else besides momentum conservation.

The quark-gluon state (35) must be orthogonal to the quark state of equation (33) and it follows that

$$\Psi_{qg\to q}(p', k \to p) = -\Psi^\dagger_{q\to qg}(p \to p', k). \tag{37}$$

In order to calculate $\Psi_{q\to qg}$ the matrix elements for $\bar{u}(p', s')\not{\epsilon}^*(k, \lambda)u(p, s)$ are needed. These can be calculated from explicit expressions for the spinors, $\gamma$-matrices and polarization vectors and are also commonly found tabulated in the literature. The matrix elements for $\frac{\bar{u}_{\sigma'}(p')}{\sqrt{p'^+}}\gamma^\mu \frac{u_\sigma(p)}{\sqrt{p^+}}$ are listed in table 1. With some algebra these can be reworked into

$$\bar{u}_{\sigma'}(p')\not{\epsilon}^*(k, \lambda)u_\sigma(p) = \frac{2\epsilon^*_\perp(\lambda) \cdot (k_\perp - zp_\perp)}{z\sqrt{1-z}}\left(\delta_{\sigma,\lambda} + \delta_{\sigma,-\lambda}(1-z)\right). \tag{38}$$

In direct contrast with the Feynman diagram method, these matrix elements contains explicit information on the helicity structure of the process. From the $\delta_{\sigma\sigma'}$'s we see that the quark helicity cannot be flipped, and the reworked matrix element (38) explicitly distinguishes between the cases where the quark and gluon have same or opposite helicity.

## 3.3 The differential cross section in terms of the transition amplitude

Following in the footsteps of Bjorken, Kogut and Soper [4], the differential cross-section is

$$\mathrm{d}\sigma = \frac{1}{2p^+}\frac{\mathrm{d}^2p'_\perp \mathrm{d}p'^+}{(2\pi)^3 2p'^+}\frac{\mathrm{d}^2k_\perp \mathrm{d}k^+}{(2\pi)^3 2k^+}(2\pi)\delta(p^+ - p'^+ - k^+)\left|\langle q(p')g(k)|\,\mathcal{T}\,|q(p)\rangle\right|^2 , \tag{39}$$

where the transition amplitude is defined by

$$\begin{aligned}\langle q(p')g(k)|\,U(\infty,0)[\mathbf{F}-1]U(0,-\infty)\,|q(p)\rangle \\ = (2\pi)\delta(p^+ - p'^+ - k^+)\,\langle q(p')g(k)|\,\mathcal{T}\,|q(p)\rangle ,\end{aligned} \tag{40}$$

and the operator $\mathbf{F}$ describing the interaction with the classical field is given by

$$\mathbf{F} = \exp\left(-i\int \mathrm{d}x^+\mathrm{d}x^-\mathrm{d}x_\perp eQA_+(x^+,0,x_\perp)\psi^\dagger(0,x^-,x_\perp)\psi(0,x^-,x_\perp)\right). \tag{41}$$

We are interested in the particular case of scattering off a Coulomb potential

$$A_0(x^+,0,x_\perp) = \frac{1}{4\pi}\frac{e}{\sqrt{z^2+x_\perp^2}} = \frac{1}{4\pi}\frac{e}{\sqrt{\frac{1}{2}(x^+)^2+x_\perp^2}}, \tag{42}$$

or more specifically

$$\begin{aligned}A_+(x^+,0,x_\perp) &= \frac{1}{\sqrt{2}}A_0(x^+,0,x_\perp) = \frac{1}{\sqrt{2}}\frac{1}{4\pi}\frac{e}{\sqrt{z^2+x_\perp^2}} \\ &= \frac{1}{\sqrt{2}}\frac{1}{4\pi}\frac{e}{\sqrt{\frac{1}{2}(x^+)^2+x_\perp^2}}.\end{aligned} \tag{43}$$

We must first evaluate the left-hand side of equation (40). We do this by first plugging in the Fock state expansions (33) and (35)

$$\begin{aligned}\langle q(p')g(k)|\,U(\infty,0)[\mathbf{F}-1]U(0,-\infty)\,|q(p)\rangle = \Big(\langle q(p')g(k)|_0 \\ + \int \mathrm{d}\Omega_2 \Psi^\dagger_{qg\to q}(p',k\to\widetilde{p})\,\langle q(\widetilde{p})|_0\Big)\,[\mathbf{F}-1]\,\Big(|q(p)\rangle_0 \\ + \int \mathrm{d}\Omega_1 \Psi_{q\to qg}(p\to\widetilde{p}',\widetilde{k})\,\left|q(\widetilde{p}')g(\widetilde{k})\right\rangle_0\Big) .\end{aligned} \tag{44}$$

Next we should study how the operator $\mathbf{F}$ acts on these Fock states.

## 3.4 Action of the operator F on Fock states

The action of the operator $\mathbf{F}$, defined in equation (41), on a Fock state turns out to be simple. Since $\mathbf{F}$ is invariant under boosts in the $x^-$ direction, it must commute with the momentum operator $p^+$ [4]. Assuming that $|0\rangle$ is the *only* Fock state with zero momentum, we get

$$\mathbf{F}\,|0\rangle = |0\rangle \tag{45}$$

because $0 = \mathbf{F}p^+\,|0\rangle = p^+\,(\mathbf{F}\,|0\rangle) = p^+\,|0\rangle$.

Acting on the general Fock state $|n_q, n_g\rangle$ of equation (28) we can transport the operator $\mathbf{F}$ past all the creation operators until it it acts on the vacuum:

$$\begin{aligned}
\mathbf{F}\,|n_q, n_g\rangle &= \mathbf{F}\prod_{i=0}^{n_q} a^\dagger(p_i, s_i)\prod_{j=0}^{n_g} b^\dagger(k_j, \lambda_j)\,|0\rangle \\
&= \prod_{i=0}^{n_q}\left[\mathbf{F}a^\dagger(p_i, s_i)\mathbf{F}^{-1}\right]\prod_{j=0}^{n_g}\left[\mathbf{F}b^\dagger(k_j, \lambda_j)\mathbf{F}^{-1}\right]\mathbf{F}\,|0\rangle \\
&= \prod_{i=0}^{n_q}\left[\mathbf{F}a^\dagger(p_i, s_i)\mathbf{F}^{-1}\right]\prod_{j=0}^{n_g}\left[\mathbf{F}b^\dagger(k_j, \lambda_j)\mathbf{F}^{-1}\right]|0\rangle\,.
\end{aligned} \tag{46}$$

Next we need to evaluate $\mathbf{F}a^\dagger(p_i, s_i)\mathbf{F}^{-1}$ and $\mathbf{F}b^\dagger(k_j, \lambda_j)\mathbf{F}^{-1}$. Using the series expansion of $\mathbf{F}$ and the anticommutator (31), we find that

$$\mathbf{F}\psi^\dagger(0, x^-, x_\perp)\mathbf{F}^{-1} = \psi^\dagger(0, x^-, x_\perp)\mathrm{e}^{-ieQ\int \mathrm{d}x^+ A_+(x^+,0,x_\perp)}. \tag{47}$$

Fourier transforming both sides of the equation and applying the convolution theorem gives

$$\mathbf{F}a^\dagger(p^+, p_\perp; s)\mathbf{F}^{-1} = \int \frac{\mathrm{d}^2\widetilde{p}_\perp}{(2\pi)^2} a^\dagger(p^+, \widetilde{p}_\perp; s)F(\widetilde{p}_\perp - p_\perp), \tag{48}$$

where

$$F(p_\perp) = \int \mathrm{d}^2x_\perp e^{-ip_\perp\cdot x_\perp}e^{-ieQ\int \mathrm{d}x^+ A_+(x^+,0,x_\perp)}. \tag{49}$$

This is a transverse Fourier transformation of a Wilson line.

By similar means it is straightforward to see that the operator has no effect on the gluon creation operator:

$$\mathbf{F}b^\dagger(k, \lambda, c)\mathbf{F}^{-1} = b^\dagger(k, \lambda, c). \tag{50}$$

Applying equations (46), (48) and (50) to equation (44) can now tackle the actual scattering. Explicitly:

$$\begin{aligned}\mathbf{F}\left|q(p)\right\rangle_0 = \mathbf{F}a^\dagger(p)\left|0\right\rangle = \mathbf{F}a^\dagger(p)\mathbf{F}^{-1}\left|0\right\rangle = \int \frac{\mathrm{d}^2\widetilde{p}_\perp}{(2\pi)^2}a^\dagger(p^+,\widetilde{p}_\perp)F(\widetilde{p}_\perp - p_\perp)\left|0\right\rangle \\ = \int \frac{\mathrm{d}^2\widetilde{p}_\perp}{(2\pi)^2}F(\widetilde{p}_\perp - p_\perp)\left|q(p^+,\widetilde{p}_\perp)\right\rangle \qquad (51)\end{aligned}$$

and

$$\begin{aligned}\mathbf{F}\left|q(p')g(k)\right\rangle_0 &= \mathbf{F}a^\dagger(p')\mathbf{F}^{-1}\mathbf{F}b^\dagger(k)\mathbf{F}^{-1}\left|0\right\rangle \\ &= \int \frac{\mathrm{d}^2\widetilde{p}_\perp}{(2\pi)^2}a^\dagger(p'^+,\widetilde{p}_\perp)F(\widetilde{p}_\perp - p'_\perp)b^\dagger(k)\left|0\right\rangle \\ &= \int \frac{\mathrm{d}^2\widetilde{p}_\perp}{(2\pi)^2}F(\widetilde{p}_\perp - p'_\perp)\left|q(p'^+,\widetilde{p}_\perp)g(k)\right\rangle . \qquad (52)\end{aligned}$$

Applying our new insight to equation (44) we get

$$\begin{aligned}&\left\langle q(p')g(k)\right| U(\infty,0)[\mathbf{F}-1]U(0,-\infty)\left|q(p)\right\rangle \\ =&\int \mathrm{d}\Omega_1\Psi_{q\to qg}(p\to\widetilde{p}',\widetilde{k})\left\langle q(p')g(k)\right|\mathbf{F}\left|q(\widetilde{p}')g(\widetilde{k})\right\rangle_0 \\ &-\int \mathrm{d}\Omega_2\Psi_{q\to qg}(\widetilde{p}\to p',k)\left\langle q(\widetilde{p})\right|\mathbf{F}\left|q(p)\right\rangle_0 \\ &-\int \mathrm{d}\Omega_1\Psi_{q\to qg}(p\to\widetilde{p}',\widetilde{k})\left\langle q(p')g(k)\middle|q(\widetilde{p}')g(\widetilde{k})\right\rangle_0 \\ &+\int \mathrm{d}\Omega_2\Psi_{q\to qg}(\widetilde{p}\to p',k)\left\langle q(\widetilde{p})\middle|q(p)\right\rangle_0 \\ =&2p^+(2\pi)\delta(k^+ + p'^+ - p^+)\left[F(p'_\perp - p_\perp + k_\perp) - (2\pi)^2\delta^2(p_\perp - k_\perp - p'_\perp)\right] \\ &\times\left[\Psi_{q\to qg}(p\to(p-k),k) - \Psi_{q\to qg}((p'+k)\to p',k)\right]. \qquad (53)\end{aligned}$$

Referring back to equation (32), the wave functions with these particular momenta as arguments are

$$\Psi_{q\to qg}(p\to(p-k),k) = g\bar{u}(p-k)\not{\epsilon}^*(k)(t^a_{ij})u(p)\frac{z(z-1)}{(zp_\perp - k_\perp)^2} \qquad (54)$$

and

$$\Psi_{q\to qg}((p'+k)\to p',k) = g\bar{u}(p')\not{\epsilon}^*(k)(t^a_{ij})u(p'+k)\frac{z(z-1)}{(z(k_\perp + p'_\perp) - k_\perp)^2}, \qquad (55)$$

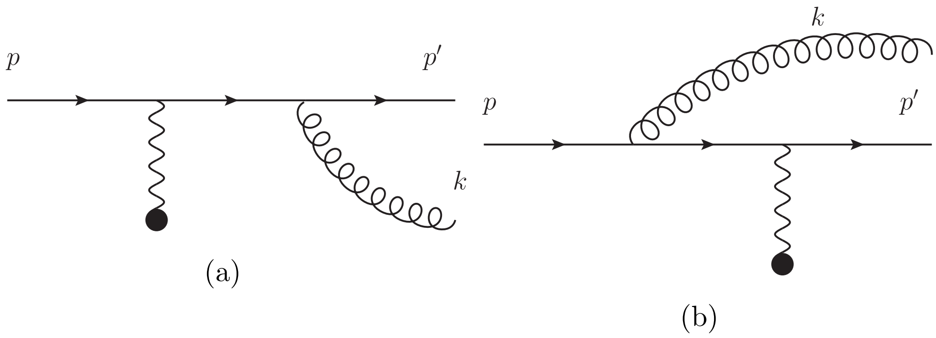


Figure 5: The two light-cone time orderings for the process at tree-level. The light-cone time flows from left to right and the black dots represent scatterings from the external field.

where we have used the on-shell condition (22), and the notation $p'^{+} = (1-z)p^{+}$, $k^{+} = zp^{+}$.

The transition amplitude related to cross-sections as defined by equation (40) is thus

$$\langle q(p')g(k)|\,\mathcal{T}\,|q(p)\rangle = 2p^{+}\left[F(p'_{\perp} - p_{\perp} + k_{\perp}) - (2\pi)^2\delta^2(p_{\perp} - k_{\perp} - p'_{\perp})\right] \times gz(z-1)\left[\frac{\bar{u}(p-k)\not{\epsilon}^*(k)(t^a_{ij})u(p)}{(zp_{\perp} - k_{\perp})^2} - \frac{\bar{u}(p')\not{\epsilon}^*(k)(t^a_{ij})u(p'+k)}{(z(k_{\perp} + p'_{\perp}) - k_{\perp})^2}\right]. \tag{56}$$

The terms in this expression can be visually represented as the diagrams in figures 5a and 5b.

## 3.5 The perturbative expansion of the distribution $F$

To evaluate the cross-section perturbatively, we expand the distribution $F$:

$$\begin{aligned} F(p_{\perp}) &= \int \mathrm{d}^2x_{\perp} e^{-ip_{\perp}\cdot x_{\perp}} e^{-ieQ\int \mathrm{d}x^{+}A_{+}(x^{+},0,x_{\perp})} \\ &\approx \int \mathrm{d}^2x_{\perp} e^{-ip_{\perp}\cdot x_{\perp}} \left(1 - ieQ\int \mathrm{d}x^{+}A_{+}(x^{+},0,x_{\perp})\right) \\ &= (2\pi)^2\delta^2(p_{\perp}) - ieQ\int \mathrm{d}^2x_{\perp} e^{-ip_{\perp}\cdot x_{\perp}} \int \mathrm{d}x^{+}\frac{1}{\sqrt{2}}\frac{1}{4\pi}\frac{e}{\sqrt{\frac{1}{2}(x^{+})^2 + x_{\perp}^2}}. \end{aligned} \tag{57}$$

To calculate the integrals one needs to employ a couple of tricks. Firstly, the integral as such is divergent and needs to be regularized. This is commonly done by introducing an exponentially damping factor $e^{-\lambda r}$, turning the Coulomb potential into a Yukawa potential. This can be interpreted as giving the photon a positive mass. The correct result is recovered by taking the limit $\lambda \to 0$ after the integration.

Secondly, the transverse Fourier transformation can be a bit of a pain to dive into straight away. It's much easier to consider the full 3-dimensional Fourier transformation and take one momentum component to zero at the end, leading to the same result.

Armed with these little tricks one gets

$$\begin{aligned}
&-ie^2Q\int \mathrm{d}^2x_\perp \mathrm{d}x^+ e^{-ip_\perp\cdot x_\perp}\frac{1}{\sqrt{2}}\frac{1}{4\pi}\frac{1}{\sqrt{\frac{1}{2}(x^+)^2+x_\perp^2}} \\
&\xrightarrow{\text{regularization}} \frac{-ie^2Q\sqrt{2}}{4\sqrt{2}\pi}\int \mathrm{d}^2x_\perp \mathrm{d}z e^{-i\mathbf{p}\cdot\mathbf{x}}\frac{e^{-\lambda\sqrt{z^2+x_\perp^2}}}{\sqrt{z^2+x_\perp^2}} \\
&= \frac{-ie^2Q}{4\pi}\int_0^\infty \mathrm{d}r\int_0^\pi \mathrm{d}\phi\int_0^{2\pi}\mathrm{d}\theta e^{-ipr\cos\phi}\frac{e^{-\lambda r}}{r}r^2\sin\phi = -ie^2Q\frac{1}{p^2+\lambda^2} \\
&\xrightarrow{\lambda\to 0} -ie^2Q\frac{1}{p^2} = \frac{-ie^2Q}{p_\perp^2}.
\end{aligned} \tag{58}$$

## 3.6 Final result for the differential cross section

Equation (56) now reads

$$\begin{aligned}
\langle q(p')g(k)|\,\mathcal{T}\,|q(p)\rangle &= -i2p^+\frac{e^2Q}{q_\perp^2}gz(z-1)\left[\frac{\bar{u}(p-k)\not{\epsilon}^*(k)(t^a_{ij})u(p)}{(zp_\perp-k_\perp)^2}\right. \\
&\left.-\frac{\bar{u}(p')\not{\epsilon}^*(k)(t^a_{ij})u(p'+k)}{(z(k_\perp+p'_\perp)-k_\perp)^2}\right] \\
&= \frac{-2ie^2Qgp^+z(z-1)}{(p'_\perp+k_\perp-p_\perp)^2}\left[\frac{\bar{u}(p-k)\not{\epsilon}^*(k)(t^a_{ij})u(p)}{(zp_\perp-k_\perp)^2}-\frac{\bar{u}(p')\not{\epsilon}^*(k)(t^a_{ij})u(p'+k)}{(z(k_\perp+p'_\perp)-k_\perp)^2}\right] \\
&= \frac{-2ie^2Q(t^a_{ij})gp^+z(z-1)}{q_\perp^2}\left[\frac{\bar{u}(p-k)\not{\epsilon}^*(k)u(p)}{(zp_\perp-k_\perp)^2}\right.
\end{aligned}$$

$$-\frac{\bar{u}(p+q-k)\not\epsilon^*(k)u(p+q)}{(z(p_\perp+q_\perp)-k_\perp)^2}\Bigg], \tag{59}$$

where $q_\perp = p'_\perp - p_\perp + k_\perp$ is the transverse momentum transferred from the external field. With the matrix elements from (38) this becomes

$$\begin{aligned}
\langle q(p')g(k)|\,\mathcal{T}\,|q(p)\rangle &= \frac{-4ie^2Q(t^a_{ij})gp^+z(z-1)}{z\sqrt{1-z}q_\perp^2}\delta_{\sigma,\sigma'}(\delta_{\sigma,\lambda}+(1-z)\delta_{\sigma,-\lambda}) \\
&\times\left[\frac{\epsilon^*_\perp(\lambda)\cdot(k_\perp-zp_\perp)}{(zp_\perp-k_\perp)^2}-\frac{\epsilon^*_\perp(\lambda)\cdot(k_\perp-z(p'_\perp+k_\perp))}{(z(k_\perp+p'_\perp)-k_\perp)^2}\right] \\
&= \frac{4ie^2Q(t^a_{ij})gp^+\sqrt{1-z}}{q_\perp^2}\delta_{\sigma,\sigma'}(\delta_{\sigma,\lambda}+(1-z)\delta_{\sigma,-\lambda})\left[\frac{\epsilon^*_\perp(\lambda)\cdot(k_\perp-zp_\perp)}{(zp_\perp-k_\perp)^2}\right. \\
&\left.-\frac{\epsilon^*_\perp(\lambda)\cdot(k_\perp-z(p'_\perp+k_\perp))}{(z(k_\perp+p'_\perp)-k_\perp)^2}\right].
\end{aligned} \tag{60}$$

We are free to choose the frame such that the incoming quark is moving along the z-direction, i.e. it has zero transverse momentum $p_\perp = 0$. In this frame the amplitude looks like

$$\begin{aligned}
\langle q(p')g(k)|\,\mathcal{T}\,|q(p)\rangle &= \frac{4ie^2Q(t^a_{ij})gp^+\sqrt{1-z}}{q_\perp^2}\delta_{\sigma,\sigma'}(\delta_{\sigma,\lambda}+(1-z)\delta_{\sigma,-\lambda}) \\
&\times\left[\frac{\epsilon^*_\perp(\lambda)\cdot k_\perp}{k_\perp^2}-\frac{\epsilon^*_\perp(\lambda)\cdot(k_\perp-zq_\perp)}{(k_\perp-zq_\perp)^2}\right].
\end{aligned} \tag{61}$$

We then have to square the amplitude and sum and average over the helicities and colors of the final and initial state, respectively:

$$\begin{aligned}
&\frac{1}{2}\frac{1}{3}\sum_{\sigma,\sigma',\lambda}|\,\langle q(p')g(k)|\,\mathcal{T}\,|q(p)\rangle\,|^2 = \frac{1}{2}\frac{1}{3}\sum_{\sigma,\sigma',\lambda}\frac{16e^4g^2Q^2(p^+)^2(1-z)}{q_\perp^4}(t^a_{ij})(t^a_{ij})^*\delta_{\sigma,\sigma'} \\
&(\delta_{\sigma,\lambda}+(1-z)^2\delta_{\sigma,-\lambda})\left[\frac{\epsilon^*_{\perp i}(\lambda)\epsilon_{\perp k}(\lambda)k_{\perp i}k_{\perp k}}{k_\perp^4}-\frac{\epsilon^*_{\perp i}(\lambda)\epsilon_{\perp l}(\lambda)k_{\perp i}(k_\perp-zq_\perp)_l}{k_\perp^2(k_\perp-zq_\perp)^2}\right. \\
&\left.-\frac{\epsilon^*_{\perp j}(\lambda)\epsilon_{\perp k}(\lambda)(k_\perp-zq_\perp)_jk_{\perp k}}{k_\perp^2(k_\perp-zq_\perp)^2}+\frac{\epsilon^*_{\perp j}(\lambda)\epsilon_{\perp l}(\lambda)(k_\perp-zq_\perp)_j(k_\perp-zq_\perp)_l}{(k_\perp-zq_\perp)^4}\right].
\end{aligned} \tag{62}$$

The color factor is, again, just $(t^a_{ij})(t^a_{ij})^* = (t^a_{ij})(t^a_{ji}) = \mathrm{Tr}[t^a t^a] = 4$. Using this and the property (25) we get

$$\begin{aligned}
\frac{1}{2}\frac{1}{3}\sum_{\sigma,\sigma',\lambda} |\left\langle q(p')g(k)\right| \mathcal{T} \left|q(p)\right\rangle|^2 &= \frac{32e^4g^2Q^2(p^+)^2(1-z)}{3q_\perp^4}(1+(1-z)^2) \\
&\times \left[\frac{k_\perp^2}{k_\perp^4} - \frac{2k_\perp\cdot(k_\perp - zq_\perp)}{k_\perp^2(k_\perp-zq_\perp)^2} + \frac{(k_\perp-zq_\perp)^2}{(k_\perp-zq_\perp)^4}\right] \\
&= \frac{32e^4g^2Q^2(p^+)^2(1-z)}{3q_\perp^4}(1+(1-z)^2)\left[\frac{1}{k_\perp^2} - \frac{2k_\perp\cdot(k_\perp-zq_\perp)}{k_\perp^2(k_\perp-zq_\perp)^2}\right. \\
&\left. + \frac{1}{(k_\perp-zq_\perp)^2}\right] \\
&= \frac{32e^4g^2Q^2(p^+)^2(1-z)}{3q_\perp^4}(1+(1-z)^2)\frac{z^2q_\perp^2}{k_\perp^2(k_\perp-zq_\perp)^2}. \qquad (63)
\end{aligned}$$

The final result for the differential cross section (39) is thus

$$\begin{aligned}
\mathrm{d}\sigma &= \frac{1}{2p^+}\frac{\mathrm{d}^2p'_\perp \mathrm{d}p'^+}{(2\pi)^3 2p'^+}\frac{\mathrm{d}^2k_\perp \mathrm{d}k^+}{(2\pi)^3 2k^+}(2\pi)\delta(p^+ - p'^+ - k^+)\frac{32e^4g^2Q^2(p^+)^2(1-z)}{3q_\perp^4} \\
&\times (1+(1-z)^2)\frac{z^2q_\perp^2}{k_\perp^2(k_\perp-zq_\perp)^2} \\
&= \frac{16e^4g^2Q^2}{3}\frac{\mathrm{d}^2p'_\perp \mathrm{d}p'^+}{(2\pi)^3 2p'^+}\frac{\mathrm{d}^2k_\perp \mathrm{d}k^+}{(2\pi)^3 2k^+}(2\pi) \\
&\times \delta(p^+ - p'^+ - k^+)\frac{z^2(1-z)(1+(1-z)^2)p^+}{q_\perp^2 k_\perp^2(k_\perp-zq_\perp)^2}. \qquad (64)
\end{aligned}$$

We see that this agrees with the result obtained in (19).

# 4 Scattering off a color charged target

The scattering with the external field was found to be simple with the quark picking up an eikonal phase factor from the Wilson line. This approach is also useful in describing scatterings from other kinds of targets. For example, a dilute hadron scattering off a dense target can be described by substituting the external field with a Color Glass Condensate, a semi-classical gluon field, describing the small-$x$ partons in the target [8, 9].

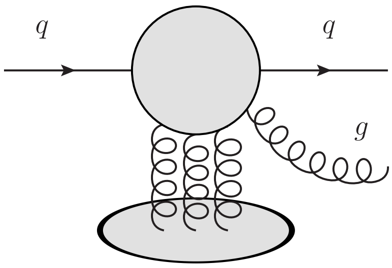


Figure 6: The bremsstrahlung process with a Color Glass Condensate target.

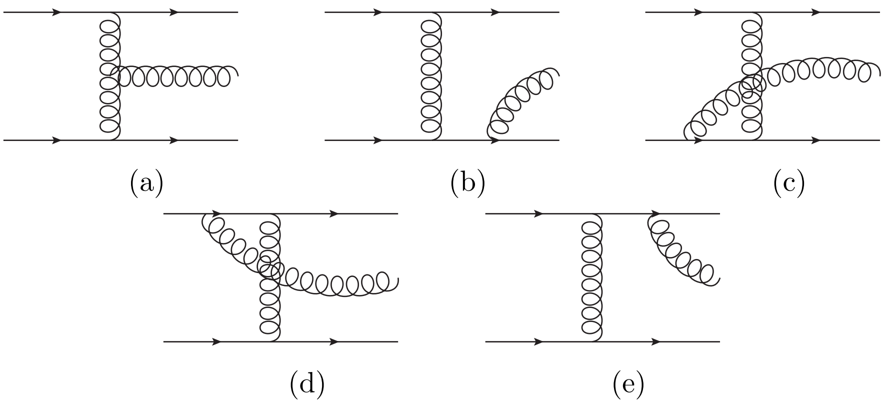


Figure 7: Graphs contributing to the bremsstrahlung process with a strongly interacting target.

A calculation with a color charged target will be complicated by the fact that the external gluon can now also be emitted from the target or the virtual gluon, leading to a larger number of graphs to be considered (see figure 7). Note, however, that diagrams 7b and 7c are suppressed in the high energy limit by the fermionic propagator from the target, for they bring in factors of $(zS)^{-1}$. In LCPT the remaining diagrams correspond to the (light-cone) time-ordered diagrams of figure 8 with only the third diagram 8c notably differing from the electromagnetic case in 5.

The non-Abelian nature of the gluon field also complicates the external scattering. If the gluon is emitted before the interaction with the target, it will also interact with the color field picking up an adjoint representation Wilson line (contrast, for example, with equation (50)). Since each adjoint Wilson line can be represented as a product of two fundamental representation Wilson lines, this leads to the presence of expectation values of products

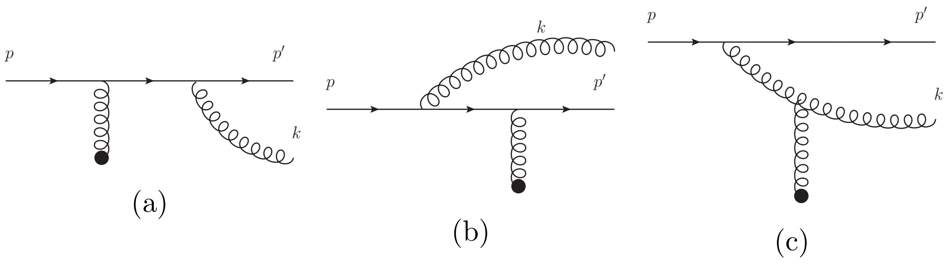


Figure 8: The leading order time-ordered diagrams for a quark-gluon dipole scattering off a color field.

of up to six non-Abelian Wilson lines in the expression for the differential cross-section [9].

Finally no exact, first principles based form for the small-$x$ color field in the target is known, so the standard procedure is to assume a Gaussian distribution of color sources within the target. The gauge field and the charge density are related by the two-dimensional Poisson equation. The gauge field is thus related to the two-dimensional massless propagator, an IR divergent quantity [9].

# 5 Concluding remarks

The results obtained in (19) and (64) are the same. This is perhaps not a trivial observation given the differences in methods used and also the fundamentally different ways of describing the external field. We see that, at very high energy, the target lepton looks just like a Coulomb field emitted by a stationary point charge.

Calculating higher order corrections to the cross-section is straightforward. The LCPT method allows for independent corrections in multiple areas of the calculation. The Fock state decompositions (33) and (35) can include more terms thus making the intermediate state scattering with the external field more complex. The light-cone wave functions (32) can be evaluated to higher orders giving a better description of each particular splitting amplitude. Finally, the eikonal Wilson line in (49) describing the scattering with the Coulomb field can be expanded beyond first order, giving the amplitudes for multiple photon scatterings.

As stated earlier, the light-cone method is at its best when calculating bound states. We have demonstrated that it is also not only usable for the calculation of cross-sections, but that it also offers additional insight into the helicity structure of the process, details easily lost when using the Lagrangian framework. At the cost of more work, the actual physics of the process is perhaps more apparent when using light-cone perturbation theory.

# References


[1] Dirac, P. A. M. *Forms of Relativistic Dynamics*. Reviews of Modern Physics Volume 21, Number 3, 1949.

[2] Brodsky, Stanley J., Pauli, Hans-Christian, Pinsky, Stephen S. *Quantum Chromodynamics and Other Field Theories on the Light Cone*. arXiv:hep-ph/9705477

[3] Kogut, John B. and Soper, Davison E. *Quantum Electrodynamics in the Infinite-Momentum Frame*. Physical Review D Volume 1, Number 10, 1970.

[4] Bjorken, James D., Kogut, John B. and Soper, Davison E. *Quantum Electrodynamics at Infinite Momentum: Scattering from an External Field*. Physical Review D Volume 3, Number 6, 1971.

[5] Kovchegov, Yuri V. and Levin, Eugene *Quantum Chromodynamics at High Energy*. Cambridge monographs on particle physics, nuclear physics and cosmology, 2012.

[6] Pauli, Hans-Christian *A Compendium of Light-Cone Quantization*. arXiv:hep-ph/0103106v1, 2001.

[7] Lepage, G. Peter and Brodsky, Stanley J. *Exclusive processes in perturbative quantum chromodynamics*. Physical Review D Volume 22, Number 9, 1980.

[8] Iancu, Edmond, Venugopalan, Raju *The Color Glass Condensate and High Energy Scattering in QCD*. arXiv:hep-ph/0303204

[9] Marquet, Cyrille *Forward inclusive dijet production and azimuthal correlations in pA collisions*. Nucl.Phys.A796:41-60,2007 arXiv:0708.0231 [hep-ph]